Reliability Engineering and Resilience 2-1 (2020) 21-49

Contents lists available at **RER**

Reliability Engineering and Resilience

Journal homepage: www.rengrj.com

High-Rise Structure Exposed to Blast Load Controls by MR Damper and Cladding Material

K.K. Kiran[1*], J.G. Kori[2]

1. Research Scholar, Government Engineering College Haveri-581101, Karnataka, India
2. Professor and Head of Civil Engineering Department, Government Engineering College Haveri-581101, Karnataka, India

Corresponding author: *kirankk0202@gmail.com*

https://doi.org/10.22115/RER.2020.213520.1016

ARTICLE INFO

Article history:
Received: 28 December 2019
Revised: 29 May 2020
Accepted: 01 September 2020

Keywords:
Blast load;
High rise structure;
MR damper;
Pressure impulse curve;
Normalized impulse curve;
Cladding material.

ABSTRACT

Blast load is an impulse, unpredictable load occurs on the structure. It causes not only damage to the structure but also takes the life of the people. Here an attempt is studied is carried out for a high-rise structure exposed to blast load. The response is calculated by using Adaptative based modal push over analysis. The responses are storey drift, displacement, velocity, accelerations, pressure, impulse, base shear, interstorey displacement, storey drift ratio and normalized pressure impulse. The three-dimensional analysis is carried out. The response is controlled by using M R damper and cladding material. The different algorithm is used for the analysis of MR damper are Bang Bang, Clipped Optimal, Lyapunov and LQR control algorithm.

1. Introduction

The unpredictable, large magnitude is blast load which acts on a structure resulting not only cause damage to the structure but also takes the life of people. The buildings such as railway stations, airports and embassies, should be designed to ensure as much safety of the occupants as possible. The load bearing structure should not collapse under any circumstances, and

How to cite this article: Kiran KK, Kori JG. High-rise structure exposed to blast load controls by mr damper and cladding material. Reliab. Eng. Resil. 2020;2(1):21–49. https://doi.org/10.22115/RER.2020.213520.1016.

progressive collapse should also be prevented. Besides, measures need to be taken to diminish the severity of the explosion (the magnitude of the pressure wave coming from epicenter of the explosion and the amount of hazardous flying debris).Blast wave is a term for the pressure and flow resulting from the rapid release of a large amount of energy in localized volume. The flow field propagating in supersonic velocities is led with a shock wave. A blast wave is generated after detonation of high explosives. The blast wave is a type of moving shock wave induced by a blast.

The main the source of load calculating the response of a structure due to blast load is pressure impulse curve. The combinations of pressure with known time is known as impulse. The curve obtained in a pressure and impulse is known as pressure impulse curve. The applications of Pi curve are used to determine the damage criteria for houses, small office building, light framed industrial building, also used to specific organs (eardrums, lungs etc) of the human body in the response of blast loading [1,2]. Theoretical and analytical method of obtaining the pressure impulse curve is shown [3,4]. A pi diagram of SDOF system for elastic plastic hardening and elastic plastic softening under the blast load is derived [5]. One of the easy, lucid, accurate method of obtain the pressure impulse curve is Energy based is shown [6].

A modified pressure impulse curve is better known as normalized pressure impulse curve. The normalized impulse curve is an important tool of the analysis of a structural member subjected to impulse load. The normalized pressure impulse curve can be easily converted into a pressure impulse curve for a given structural member with a minimum impulse and minimum peak reflected pressure asymptotes. The structural member which is subjected to vented and unvented confined blasts, where pulse load shapes are considered, a normalized pressure impulse diagram is drawn. Table 1 shows the significance of pressure impulse curve for the response of a human body.

Table 1
Overpressure effects on human bodies [7].

Sl no	Human Body effect	Peak over pressure (kPa)
1	Eardrum damage at 1% affected	16.5
2	Eardrum damage at 10% affected	19.3
3	Eardrum damage at 50% affected	34.5
4	Lung damage threshold	43.4
5	Fatal injuries at 1% affected	100
6	Fatal injuries at 10% affected	120.7
7	Fatal injuries at 50% affected	141.3
8	Fatal injuries at 90% affected	175.8
9	Fatal injuries at 99% affected	200

Twenty-five story high rise structure of irregular plan and elevations is considered. The response is calculated by using adaptative based modal push over analysis. Three dimensional is considered that is X direction, Y direction and Torsion. The blast load consists of two waves acting on a structure. The responses in terms of displacement, velocity and accelerations is

considered. The response is controlled by using Cladding material, MR damper. The pressure impulse curve is also plotted. The three-dimensional analysis is also analysed.

2. 25 Stories structural modelling exposed to blast load

High rise of 25 story structure, unsymmetrical both elevations and plan is shown in Figure The following assumptions are considered for the problem

i. Three-dimensional analysis is considered. One is X directions, second is Y directions and third is torsion.
ii. Structure is plastic material of steel.
iii. Ground accelerations is neglected
iv. Structure is subjected to blast load by considering two waves.
v. Blast load is acting on the surface, not on the air.

Figure 1 shows the plan, elevation of the structure system. The L shape plan having 9 m on the rear side and 6m on the front side, having width of 9m on the left side and 2m on the right side. First fifteen story structure is unsymmetrical and remaining ten story structure is symmetrical.

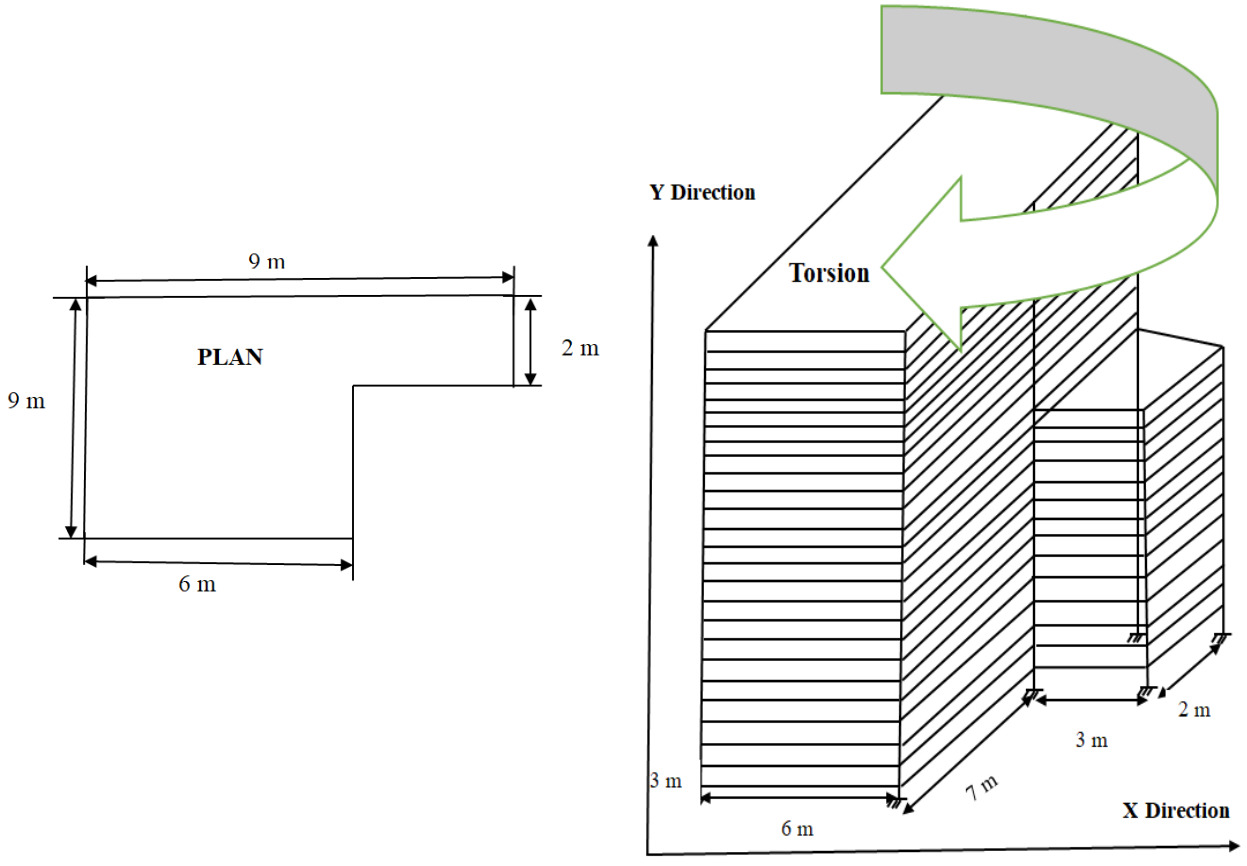

a. Plan of the unsymmetrical structure b. Elevations of the unsymmetrical structure.

Fig. 1. Plan and elevations of the 25 stories unsymmetrical structure.

Table 2 shows the dynamic properties of a structural system of various floors. It includes mass, stiffness and damping of the various floor. Table 3 shows the blast load parameter of the structure system.

Table 2
Dynamic properties of a structural system [8].

Floor	Mass (10^3 kg)	Stiffness (kN/m)	Damping (kNs/m)
1	2041	172255	27318
2	2011	156541	24826
3	2011	131956	20927
4	2011	119869	19010
5	2011	111175	17631
6	2011	102413	16241
7	2011	913068	14480
8	2011	818123	12974
9	2011	761873	12082
10	2011	713378	11313
11	2011	668616	10603
12	2011	622953	9879
13	2011	560090	8882
14	2011	512098	8121
15	2011	473719	7513
16	2011	436525	6923
17	2011	398817	6325
18	2011	359101	5695
19	2011	315938	5010
20	2011	271092	4299
21	2011	224212	3556
22	2011	177431	2814
23	2011	125646	1993
24	2011	67355	1068
25	2011	62453	986

Table 3
Blast load Parameter [7].

Sl no	Parameter	Symbol	Magnitude
1	Weight	W	1000 kg
2	Range	R	20.72 m
3	Scaled distance	Z	364.085kg/$m^{1/3}$
4	Peak reflected pressure	P_{ref}	331 kPa
5	Impulse	I	3.485 kPamsec

Figure 2 shows the blast load acting on the structure system. It consists of two waves, first wave acting on the top of the building and second wave is acting on the middle of the structure.

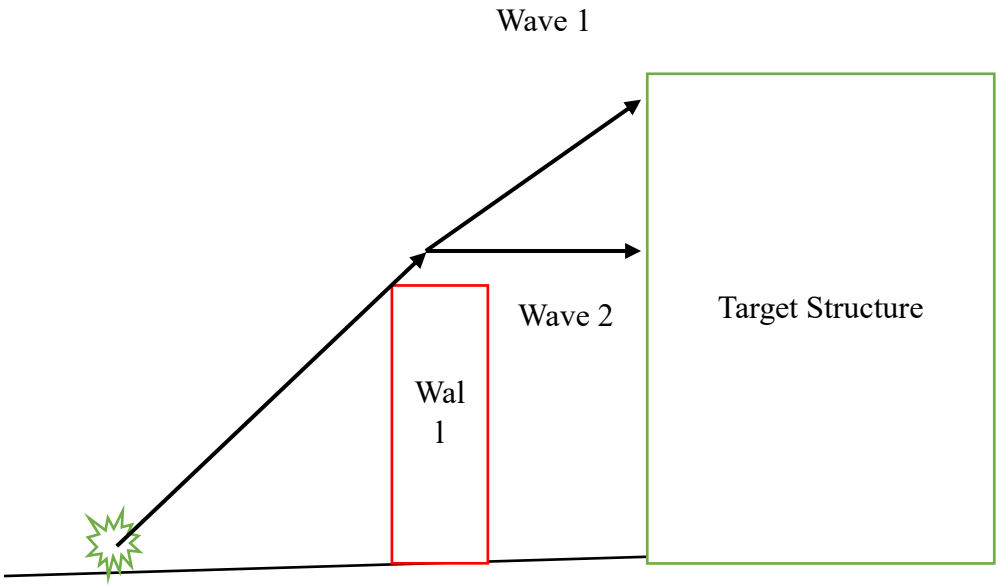

Fig. 2. Blast load acting on the structure [9].

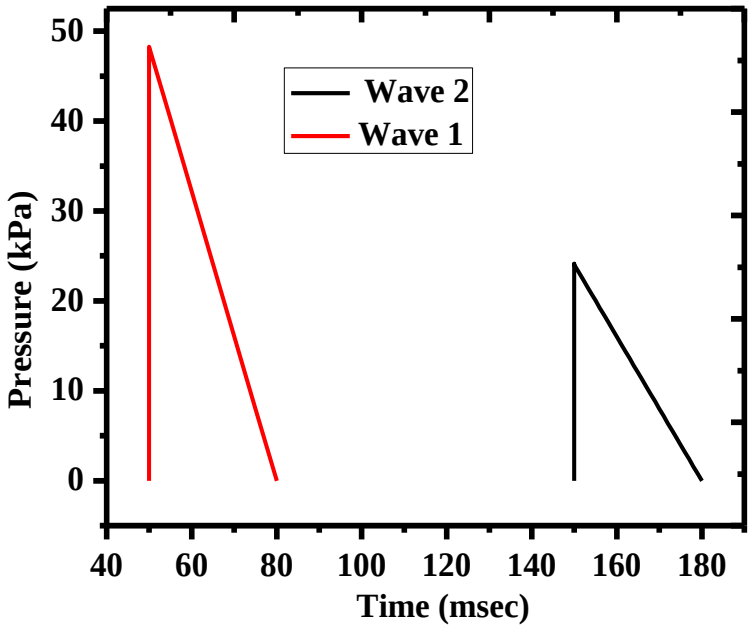

Fig. 3. Blast load on a structural system [9].

Figure 3 shows the blast load acting on the structure system. The first wave is having maximum pressure of 48 kPa at 55 msec, second wave is having maximum pressure is 25kPa at 160 msec.

The blast load parameter is calculated from the following equations

The surface blast wave parameter procedure of determining is as follows

Step 1: W is find out

Step 2: stand-off distance is determined (R_h)

$$R_h = \left(R_G{}^2 + h^2\right)^{1/2} \tag{1}$$

Step 3: Determine the scaled stand-off distance

Here Z_h- Scaled standoff distance, R_G- Scaled standoff distance, h-height of each floor

$$Z_h = {R_h}/{W^{1/3}} \tag{2}$$

Step 4: Finding the peak reflected over pressure P_r, pressure over peak incident P_{so}, time arrival t_A, duration of positive time t_o, velocity wave U by using the following equations

$$P_{so} = \frac{1.772}{Z_h{}^3} - \frac{114}{Z_h{}^2} + \frac{108}{Z_h} \tag{3}$$

$$t_o = W^{1/3} 10^{[-2.75+0.27\log(Z_h)} \tag{4}$$

$$U = a_o \cdot \sqrt{\frac{6P_{so}+7P_o}{7P_o}} \tag{5}$$

$$t_A = \frac{R_h}{U} \tag{6}$$

$$P_r = C_r . P_{so} \tag{7}$$

$$C_r = 3\left(\sqrt[4]{\frac{P_s}{101}}\right) \tag{8}$$

$$P(t) = P_o + P_r\left(1 - \frac{t}{t_o}\right)\exp\left(-\gamma\frac{t}{t_o}\right) \tag{9}$$

$$\gamma = Z_h{}^2 - 3.7Z_h + 4.2 \tag{10}$$

P(t) –time in pressure; γ-Rate wave amplitude parameter controlled, Pr- Over pressure peak reflected, P_{so} –Over pressure peak incident, t_A- Arrival of time, t_o-Duration of positive, U- wave velocity, P_o- ambient air pressure, a_o- speed of sound in air335 m/sec.

3. Cladding material

The triangular pulse shape is the blast load. The following equation gives the blast load

$$p(t) = \begin{cases} p_o\left(1 - \frac{t}{t_o}\right) & for\ t \le t_o \\ 0 & for\ t > t_o \end{cases} \tag{11}$$

p_o- blast load of intial peak pressure, t_o – load time.

Elastic equivalent motion of equation system is expressed as

$$C_m m\ddot{y} + C_s ky = C_l p(t)A \tag{12}$$

where m and k =Structure mass and stiffness of total; p(t)=Structure uniform pressure; A=blast load area of bearing; and C_m, C_s and C_l = mass, stiffness and load factors respectively. C_{lm}= C_m/C_l is the load mass factor. Equivalent mass $m_{se} = C_{lm} m$ and stiffness and load mass are same $C_s = C_l$.

$$m_{se}\ddot{y} + ky = p(t)A \tag{13}$$

The foam layer mass of densified layer is expressed as

$$\Delta m = \frac{\rho A}{\varepsilon_D}(u - y) \tag{14}$$

Where u is the cover plate displacement, y is the structure of deflection and ρ foam material density.

$$\sigma_D = \sigma_0 + \frac{\rho}{\varepsilon_D}(\dot{u} - \dot{y})^2 \tag{15}$$

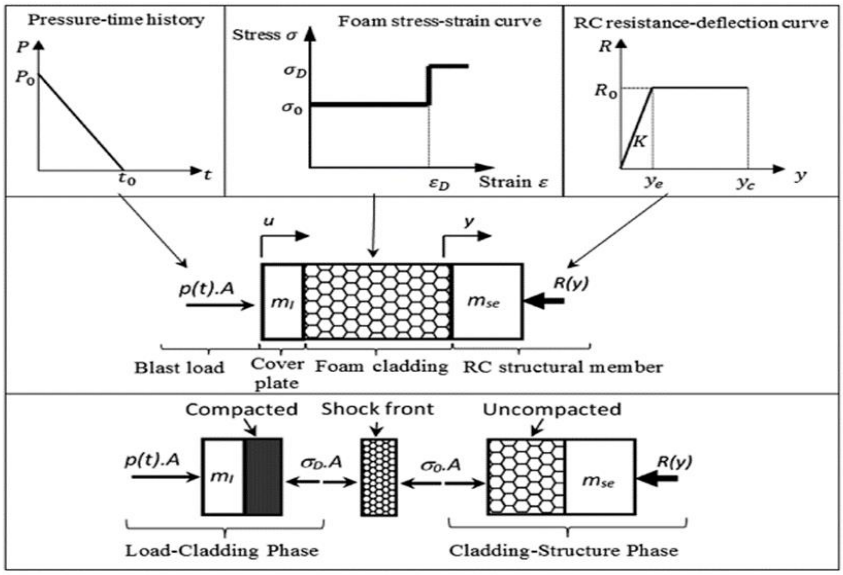

Fig. 4. Load-Cladding structure model.

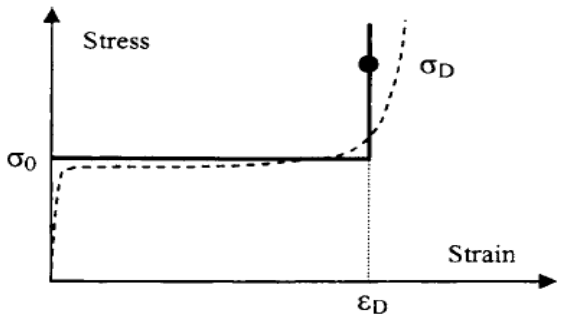

Fig. 5. Foam material of rigid perfectly plastic material.

Figure 4 show RPPL material of the foam material with plateau stresses of σ_o, at the foam locks into a rigid solid stress rises to σ_D and strain of ε_D,

The equation of motion can be express as

$$\left[m_f - \frac{\rho A}{\epsilon_D}(u - y) + m_{se}\right] y + R(y) \ddot{-} \sigma_0 A = 0 \tag{16}$$

From equation (16) can be rewritten as

$$\left[m_l + \frac{\rho A}{\varepsilon_D}(\dot{u} - \dot{y})\right] \ddot{u} + \frac{\rho A}{\varepsilon_D}(\dot{u} + \dot{y})^2 + [\sigma_o - P(t)]A = 0 \tag{17}$$

m_l= cover plate mass; u=Cladding; displacement y=RC structural member displacement; A = Crossesctional area; ε_D= Foam of densification strainand ρ=density of the foam.

After the shock load to the structure the foam is in the undensified phase. This part of the foam moves together with the main structure, which has an equivalent mass of m_{se}. the dynamic equation for the undensified phase is produced and can be expressed as

$$\left[m_f - \frac{\rho A}{\epsilon_D}(u - y) + m_{se}\right] y + R(y) \ddot{-} \sigma_0 A = 0 \tag{18}$$

m_f= foam cladding mass and $\frac{\rho A}{\varepsilon D}$(u-y) function densified part of the mass foam cladding. Fully compacted foam cladding equations can be written as

$$\left[m_l + m_f + m_{se}\right] \ddot{y} + R(y) - P(t)A = 0 \tag{19}$$

Figure 6 shows the general representations of the structures installed by cladding material. Here M_1, M_2, M_n are the mass in first floor, second floor and n^{th} floor. Table 4 shows the parameter used in the cladding material.

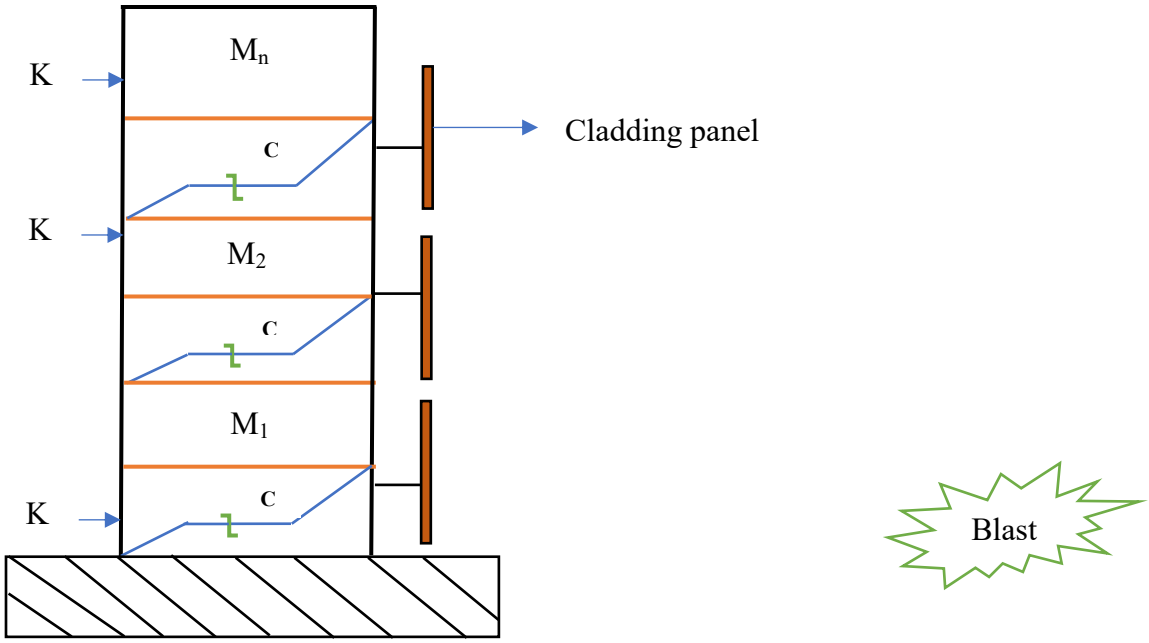

Fig. 6. Blast load acting on the structure protected by using cladding material.

Table 4
Properties of a cladding material [10].

Sl no	Parameter	Symbol	Magnitude
1	Density	ρ_c	2687 kg/m^3
2	Plateau stress	σp	444 kPa
3	Youngs Modulus	E	6.16 Mpa
4	Densification strain	ε	0.64

4. MR damper

MR damper is a semi active device used to control the vibrations of the structure. It consumes less power. It is required to estimate the electric current required to need of the device. Figure xx shows the working principal of the MR damper. The blast pressure is exerted on the structure is acting on the MR damper, then control algorithm exerted a force which acting on the structure, so that response is controlled.

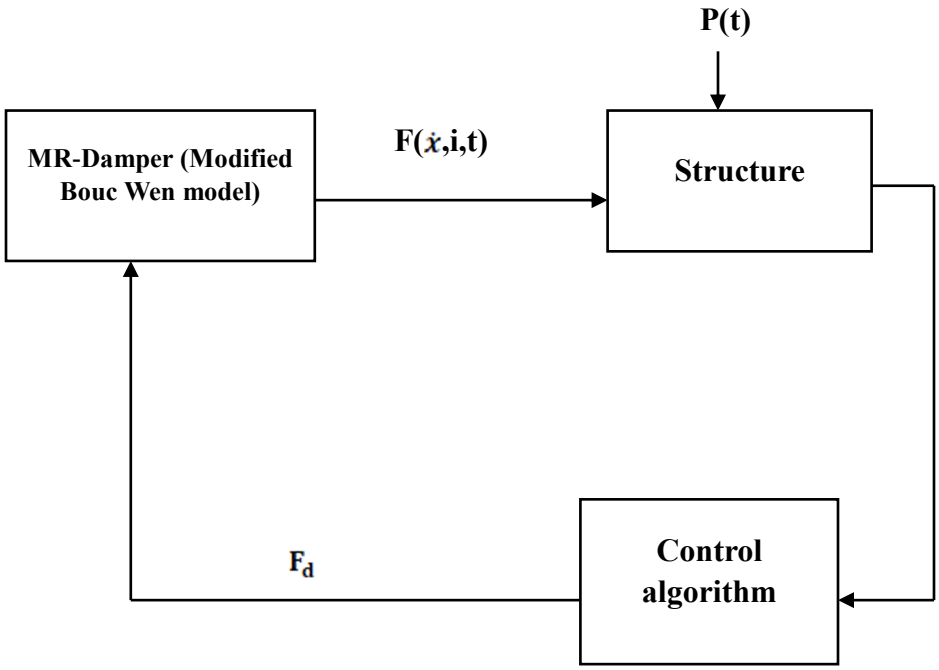

Fig. 7. MR damper model algorithm [11].

Figure 7 shows the algorithm of the MR damper principal of a structural system installed in a structure. The force required for the MR damper is calculated below equations. $F(x,i,t)$ is the force exerted by the MR damper and is the function of velocity, time and current.

$$F(x,i,t) = c_1 y + k_1(x - x_o) \tag{20}$$

Here $\dot{x}$ and x are the damper velocity and displacement (displacement and velocity of the storey where MR damper is attached). MR damper initial displacement is x_o. The other parameters in eq9 can be defined as

$$\dot{y} = \frac{1}{(c_o + c_1)}[\alpha Z + c_o \dot{x} + k_o(x - y)] \tag{21}$$

$$\dot{u} = -\eta(u - i) \tag{22}$$

$$\dot{z} = -\Upsilon\left|\dot{x} - \dot{y}\right| z\left|z\right|^{n-1} - \beta\left|\dot{x} - \dot{y}\right|\left|z\right|^{n} + A(\dot{x} - \dot{y}) \tag{23}$$

Υ, β, η and α are adjustable parameters for controlling the linearity and the behaviour of the MR damper before and after yielding. The following equations are used for LQR control algorithm

$$F_d(t) = -R_c^{-1} B^T P(t) \tag{24}$$

P(t) is the Riccati matrix.

The governing equations MR damper modal are

$$f = c_1\dot{y} + k_1(x_d - x_o) \tag{25}$$

$$\dot{Z} = -\gamma|\dot{x_d} - \dot{y}|Z|Z^{n-1}| \quad - \beta(\dot{x_d} - \dot{y})|Z^n| + \mathrm{A}(\dot{x_d} - \dot{y}) \tag{26}$$

Solving the above equation, $\dot{y}$ gives

$$\dot{y} = \frac{1}{(c_o + c_{vl})}\{\alpha Z + c_o \dot{x_d} + k_o(x_d - y)\} \tag{27}$$

where z is the evolutionary variable that accounts for the history dependence of the response, x_d is the damper displacement, $\dot{x_d}$ is the velocity across the damper, k_{al} is the accumulator stiffness, c_{vl} is the viscous damping at the lower velocity of the model to produce the roll-off, c_o is the viscous damping at larger velocity, k_o is the stiffness of the larger velocity and x^i is the initial displacement of the spring and α, β, γ , n and A are the shape or characteristic parameters of the model.

The model parameters α, c_o and c_{vl} depend on the voltage to the current driver as follows

$$\alpha = \alpha_a + \alpha_b u,\ c_o = c_{0a} + c_{0b} u \text{ and } c_{vl} = c_{la} + c_{lb} u \tag{28}$$

While the filtered voltage u determined by the applied voltage v to the control circuit is as follows

$$\dot{u} = -\eta(u - v) \tag{29}$$

The governing equations of multi storied structures with semi active M.R. damper are

$$M\ddot{x}+C\dot{x} + Kx + \Lambda F = -M\Gamma P \tag{30}$$

Where M is the mass matrix, C is the damping matrix, K is the stiffness matrix, x is the vector floor displacement, $\dot{x}$ and $\ddot{x}$ are the floor velocity and acceleration vectors respectively, Λ is a matrix of zeros and ones, where one will indicate where MR damper force is being applied, F =[$f_{d1,}$ f_{d2},.....n]^T is the vector of the control force produce by the damper, Γ is the influence coefficient vector of ones and P pressure due to blast load. For the uncontrolled case, the force F produced by the MR damper is zero.

$$\dot{Z}=Az + BF + E P \tag{31}$$

$$Y=C_c z +DF+v \tag{32}$$

Where z=[x $\dot{x}$]^T is the state vector, y=[$\ddot{x}$ x]^T is the vector of measured outputs and v is the measurement noise vector. The system of matrices are defined as follows

$$A=\begin{bmatrix} 0 & I \\ -M^{-1}K & -M^{-1}C \end{bmatrix}, B=\begin{bmatrix} 0 \\ M^{-1}\Lambda \end{bmatrix}, E=\begin{bmatrix} 0 \\ \gamma\Gamma \end{bmatrix} \tag{33}$$

$$C_c=\begin{bmatrix} -M^{-1}K & -M^{-1}C \\ I & 0 \end{bmatrix}, D=\begin{bmatrix} -M^{-1}\Lambda \\ 0 \end{bmatrix} \tag{34}$$

There are various types of control algorithm of MR damper, they are Bang Bang control algorithm, Lyapunov Stability control algorithm and clipped optimal control algorithm.

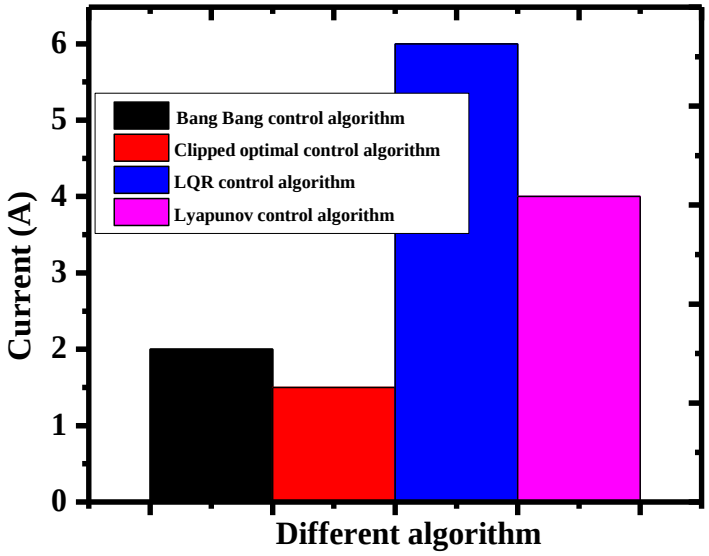

Fig. 8. Electric current requirement for various control algorithm of MR damper.

Table5
Optimizations of MR damper position in different floor.

Sl no	Combinations of floors	Percentage of reductions of response
1	1 and 2	40
2	2 and 3	32
3	1 and 3	35
4	4 and 5	30
5	6 and 3	12
6	2 and 3	24
7	1 and 4	22
8	2 and 3	18
9	4 and 6	20
10	5 and 6	17

Figure 8 shows the electric current required for the MR damper of different algorithm. The maximum electric current required for LQR control algorithm and minimum is required for Clipped optimal control algorithm. Table 5 shows the optimizations of MR damper position installed in various floors.

5. Results and discussions

Figure 9 shows the reductions of accelerations of a structural system along x direction by using MR damper and cladding material. The maximum accelerations occurs at 3rd and 20th floor of 27 m/msec^2 and 25 m/msec^2 , is reduced of 7 m/msec^2, 3.8 m/msec^2 , 3.2 m/msec^2 and 2.8 m/msec^2 at 3rd floor, ism reduced of 6 m/msec^2, 3.4 m/msec^2 , 2.4 m/msec^2 and 2.2 m/msec^2 by cladding material, Bang Bang control algorithm, clipped optimal control algorithm and Lyapunov control algorithm respectively and accelerations of a structural system along y direction by using MR damper and cladding material. The maximum accelerations occurs at 2nd and 19th floor of 18 m/msec^2 and 16 m/msec^2, is reduced of 13 m/msec^2, 12 m/msec^2 , 10 m/msec^2 and 8 m/msec^2 at 2nd floor, is reduced of 12 m/msec^2, 9 m/msec^2 , 9 m/msec^2 and 8 m/msec^2 by cladding material, Bang Bang control algorithm, clipped optimal control algorithm and Lyapunov control algorithm respectively at 19th floor.

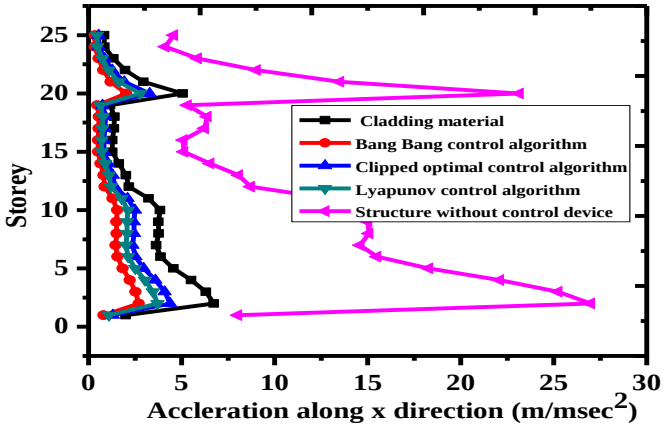

(a). 2D representation of reduction of accelerations by control devices

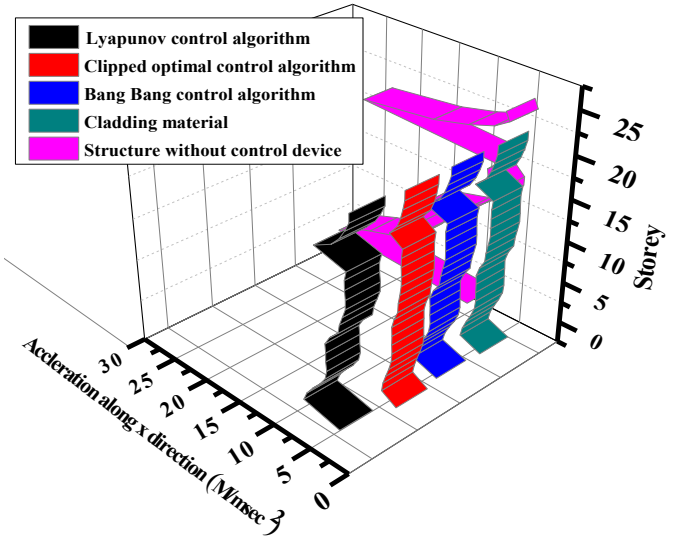

(b). 3D representation of reduction of accelerations by control devices

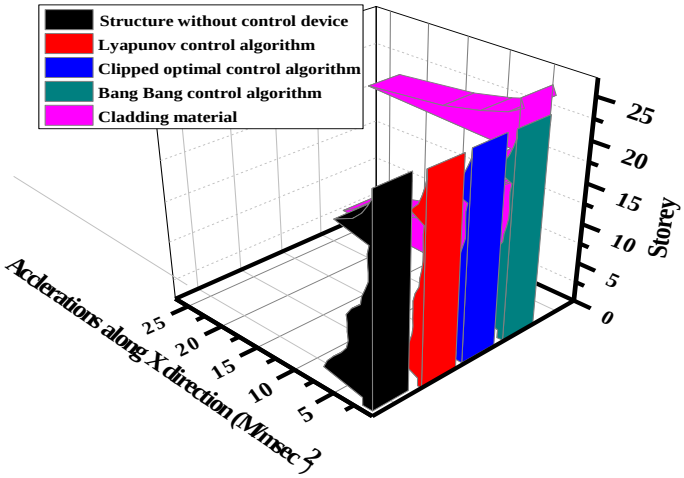

(c). 3D representation of reduction of accelerations by control devices

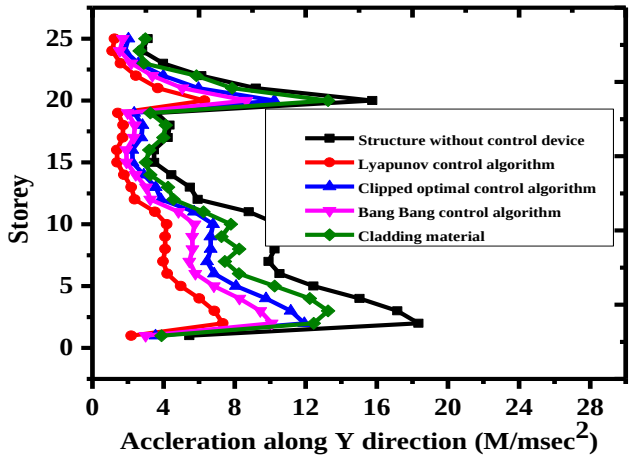

(d). 2D representation of reduction of accelerations by control devices

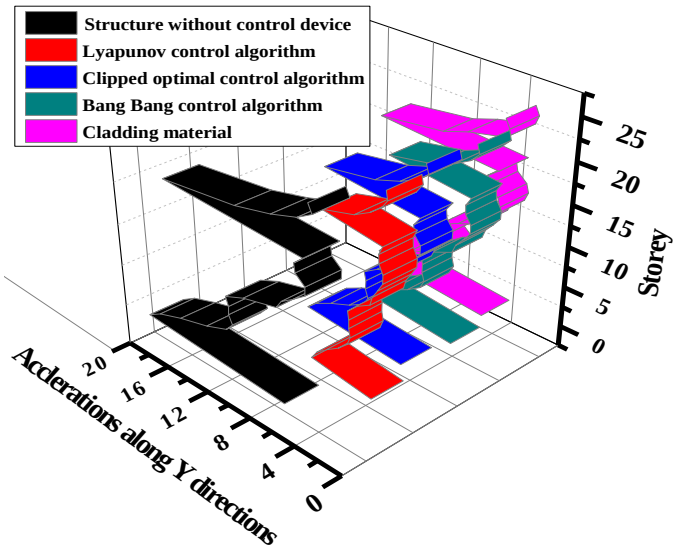

(e). 3D representation of reduction of accelerations by control devices

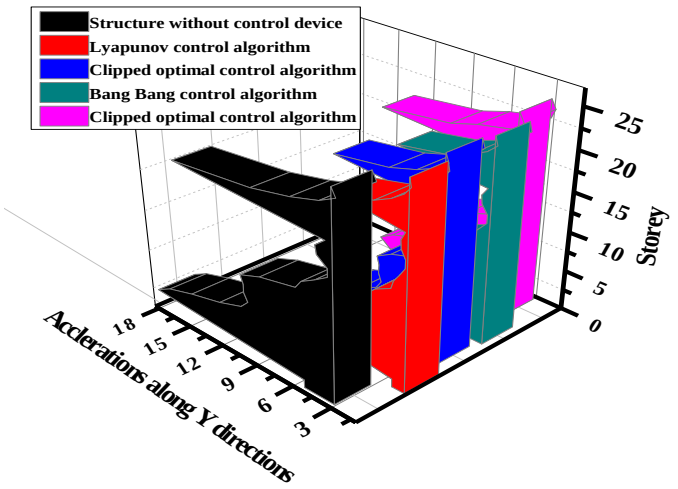

(f). 3D representation of reduction of accelerations by control devices

Fig. 9. Reduction of accelerations of structural system by control device along x and y directions.

Figure 10 shows the reductions of velocity of a structural system along x direction by using MR damper and cladding material. The maximum velocity occurs at 3rd and 21th floor of 2 m/msec and 1.7 m/msec , is reduced of 1.25 m/msec, 1 m/msec , 0.6 m/msec and 0.5 m/msec at 3rd floor, is reduced of 1 m/msec, 0.9 m/msec , 0.5 m/msec and 0.48 m/msec by cladding material, Bang Bang control algorithm, clipped optimal control algorithm and Lyapunov control algorithm respectively and velocity of a structural system along y direction by using MR damper and cladding material. The maximum velocity occurs at 2nd and 22 nd floor of 18 m/msec and 16 m/msec, is reduced of 12m/msec, 3 m/msec , 2.4 m/msec and 2 m/msec at 2nd floor, is reduced of 12 m/msec, 3 m/msec , 2.4 m/msec and 2.1 m/msec by cladding material, Bang Bang control algorithm, clipped optimal control algorithm and Lyapunov control algorithm respectively at 2 nd floor.

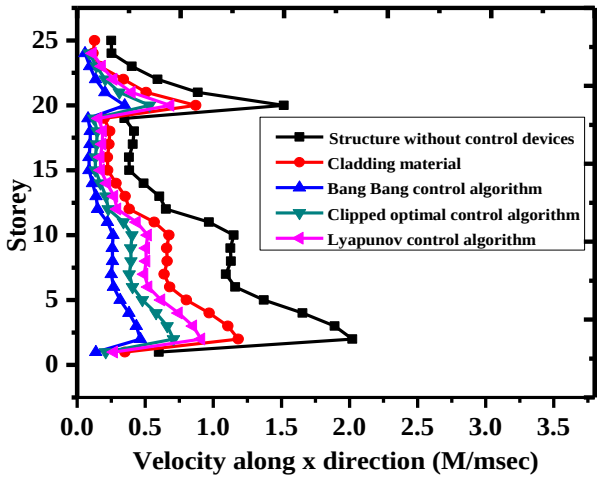

(a). 2D representation of reduction of velocity by control devices

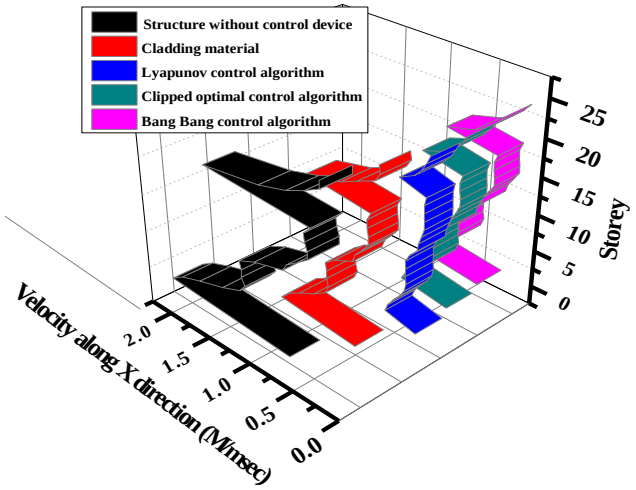

(b). 3D representation of reduction of velocity by control devices

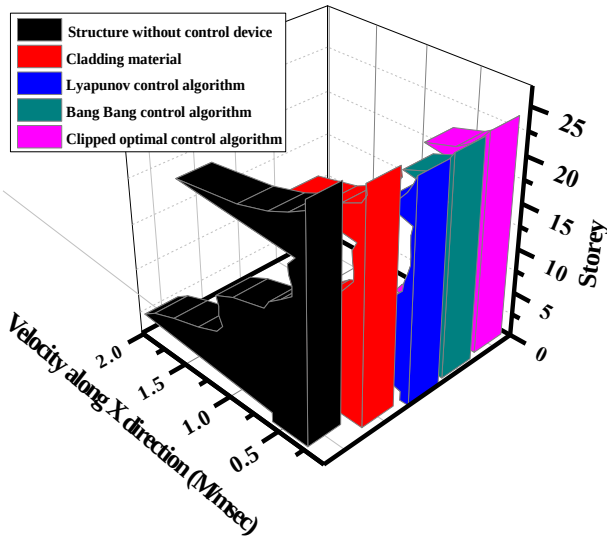

(c). 3D representation of reduction of velocity by control devices

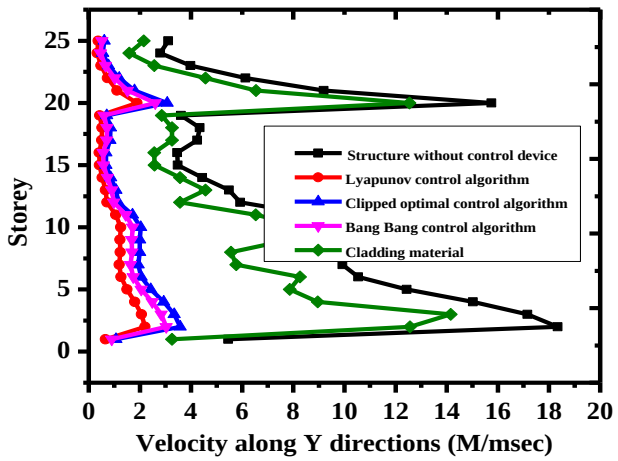

(d). 2D representation of reduction of velocity by control devices

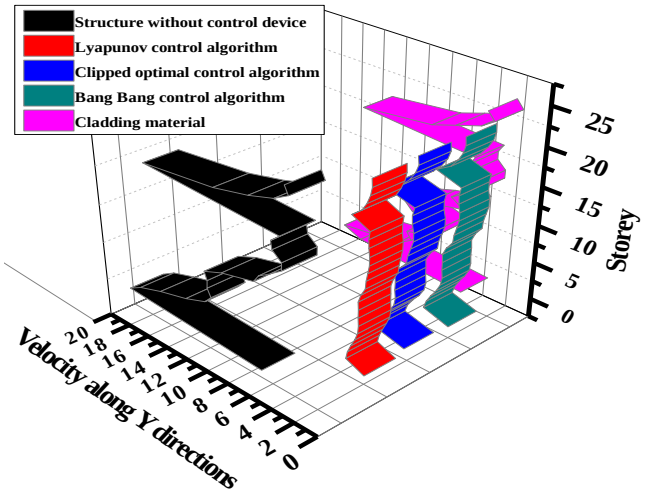

(e). 3D representation of reduction of velocity by control devices

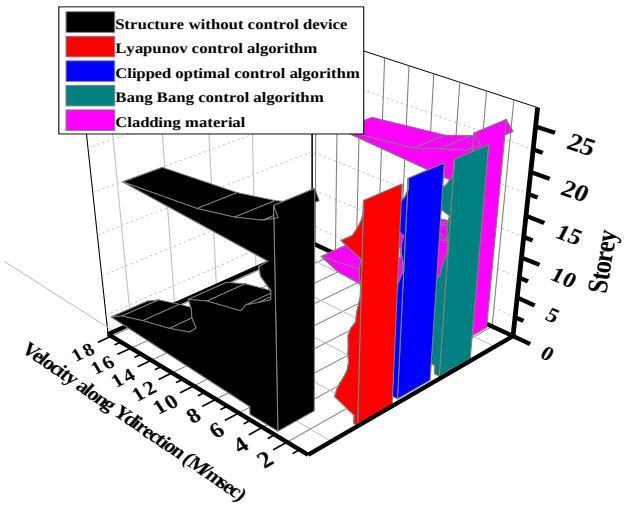

(f). 3D representation of reduction of velocity by control devices

Fig. 10. Reduction of velocity of structural system by control device along x and y directions.

Figure 11 shows the reductions of displacement of a structural system along x direction by using MR damper and cladding material. The maximum displacement occurs at 2nd and 20th floor of 2.5 m and 2 m , is reduced of 0.6 m, 0.4 m , 0.2 m and 0.1 m at 2nd floor, is reduced of 0.5 m, 0.45 m , 0.25 m and 0.15 m by cladding material, Bang Bang control algorithm, clipped optimal control algorithm and Lyapunov control algorithm respectively and reductions of displacement of a structural system along y direction by using MR damper and cladding material. The maximum displacement occurs at 3rd and 22nd floor of 18 m and 16 m, is reduced of 12 m, 3 m, 2.8 m and 2 m at 3rd floor, is reduced of 13m, 4 m, 3.8 m and 2 m by cladding material, Bang Bang control algorithm, clipped optimal control algorithm and Lyapunov control algorithm respectively at 22nd floor.

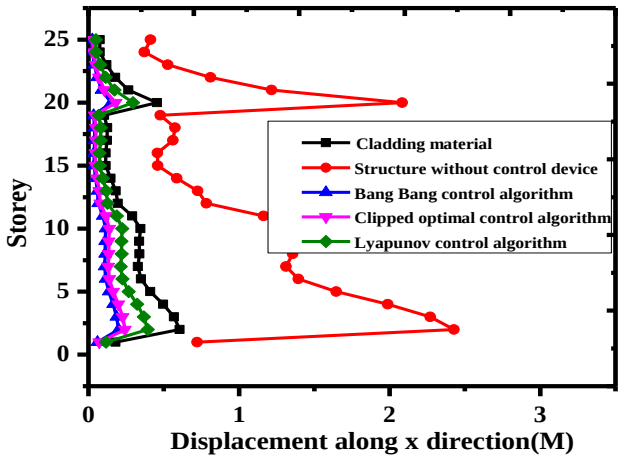

(a). 2D representation of reduction of displacement by control devices

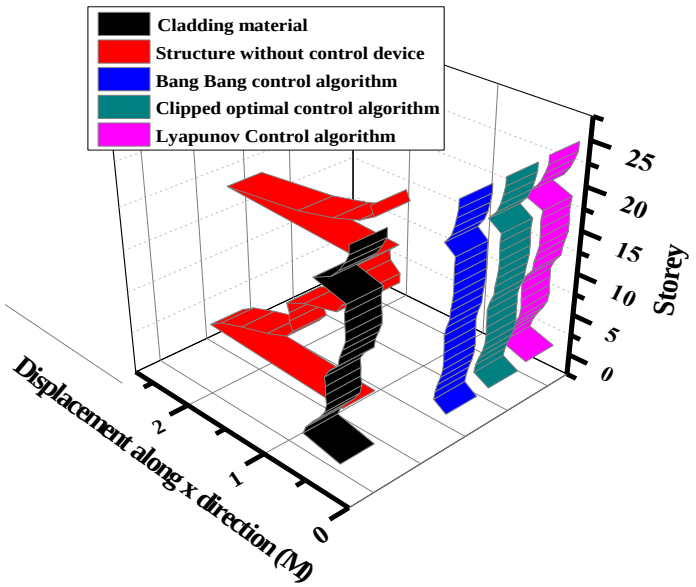

(b). 3D representation of reduction of displacement by control devices

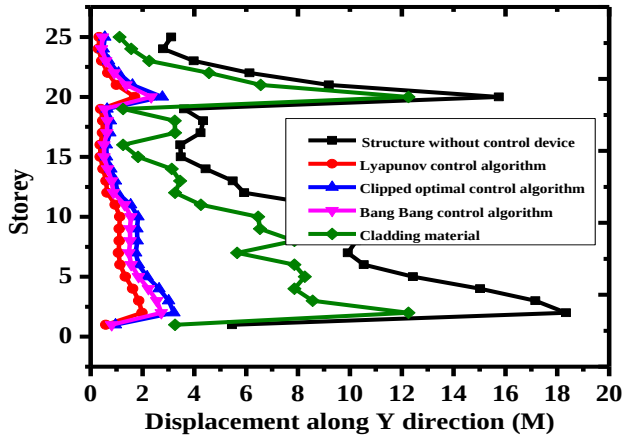

(c). 2D representation of reduction of displacement by control devices

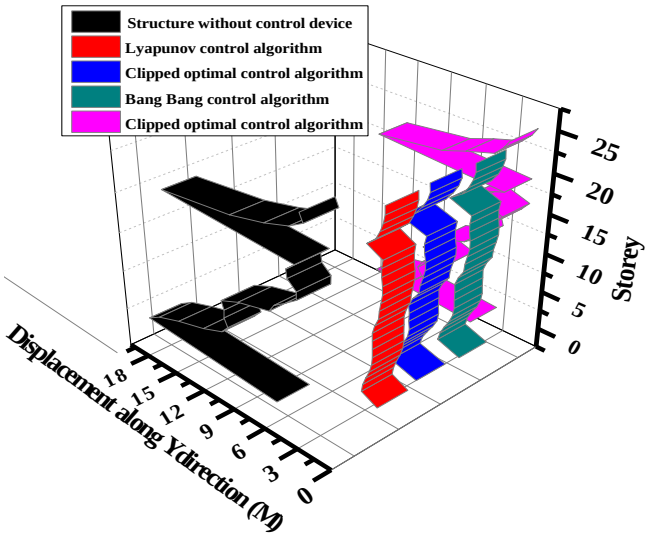

(d). 3D representation of reduction of displacement by control devices

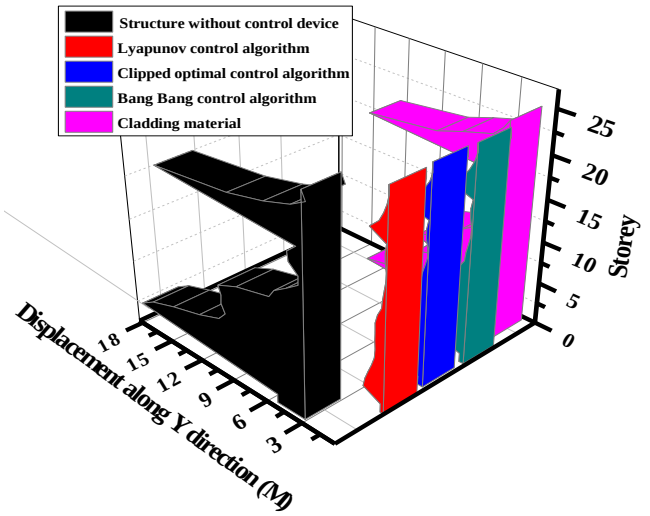

(e). 3D representation of reduction of displacement by control devices

Fig. 11. Reduction of displacement of structural system by control device along x and y directions.

Figure 12 shows the increase in pressure impulse by using cladding and MR damper without causing failure to the structure. Sixteenth floor pressure 6 kPa is increases to 11 kPa, 10kPa, 9 kPa and 7kPa by using Lyapunov control algorithm, clipped optimal control algorithm and cladding material and impulse 0.25 kPa msec to 0.38 kPa msec, 0.35 kPa msec, 0.23 kPa msec and 0.8 kPamsec. Fourth floor pressure 6.1 kPa to 10.5 kPa, 7kPa,8kPa and 6.5kPa and impulse 0.2 kPa msec to 0.39 kPa msec, 0.36 kPa msec, 0.28kPamsec and 0.24 kPa msec by using Lyapunov control algorithm, clipped optimal control algorithm and cladding material respectively.

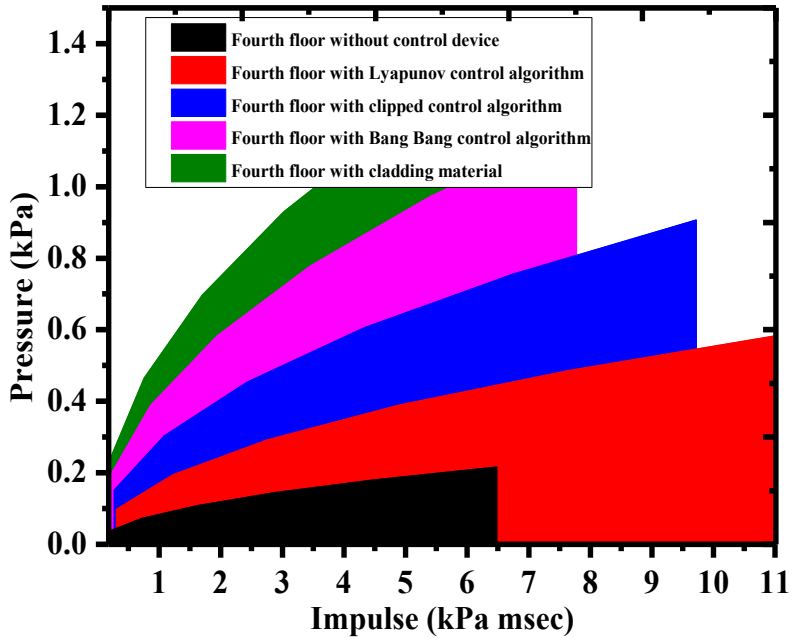

(a). 3D representation of increase of pressure impulse curve of fourth floor by control devices

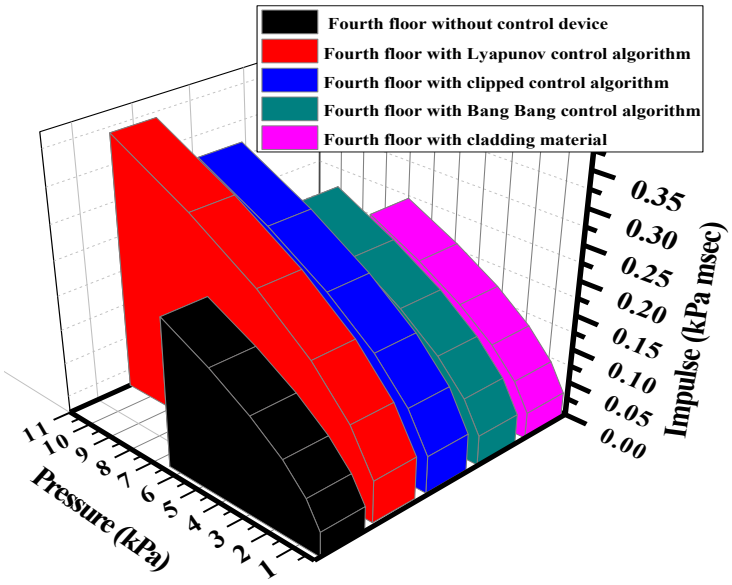

(b). 3D representation of increase of pressure impulse curve of fourth floor by control devices

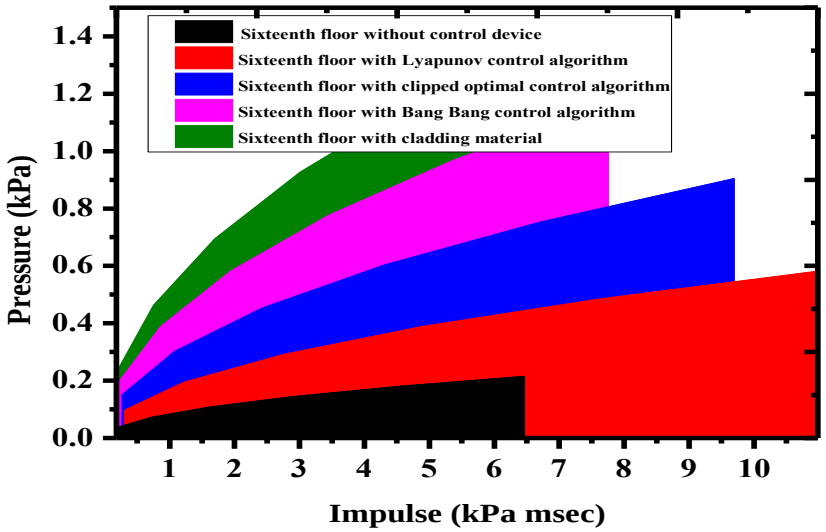

(c). 3D representation of increase of pressure impulse curve of Sixteenth floor by control devices

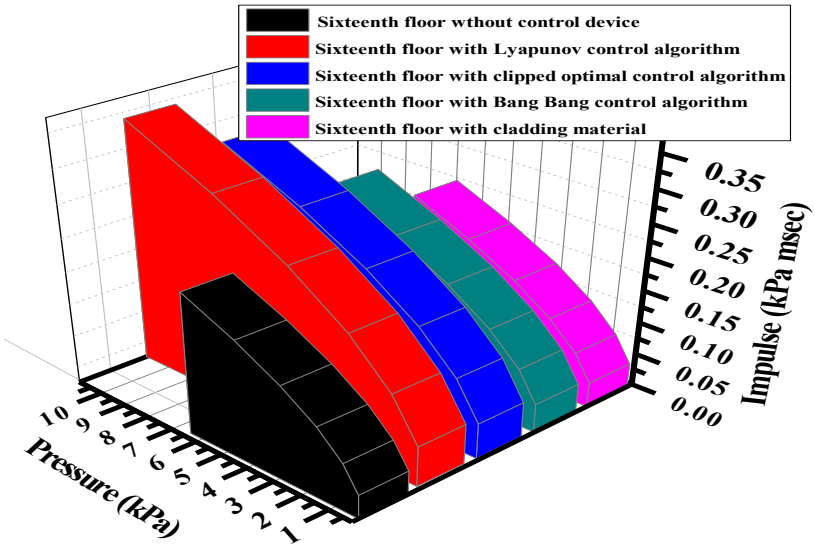

(d). 3D representation of increase of pressure impulse curve of Sixteenth floor by control devices

Fig. 12. Increase of pressure impulse curve of a structural system by using control device.

Figure 13 shows that by using cladding material interstorey displacement along x and y direction is reduced from 0.4m, 0.3m to 0.085m and 0.094m.

Figure 14 shows the reduction of the story drift by using M.R. damper of different algorithm from 0.09m to 0.085m, 0.08m and 0.078m and 1m to 0.078m, 0.6m and 0.38m at first floor along x and y direction respectively.

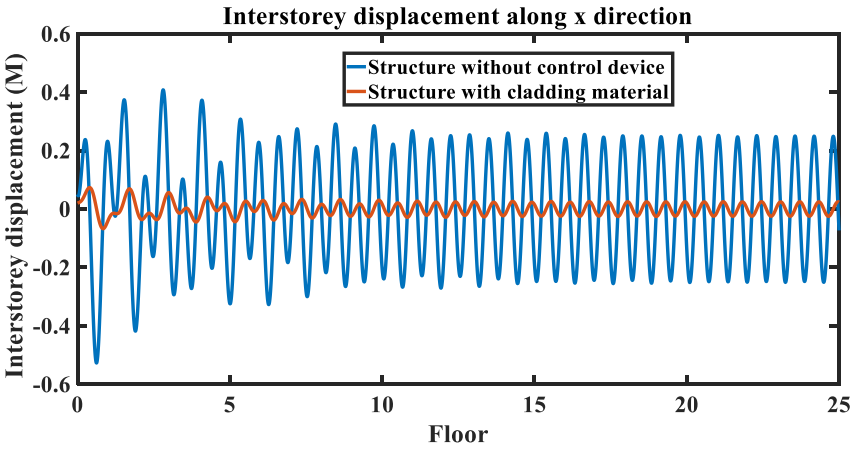

(a). Reduction of interstorey displacement of structural system by using cladding material along x directions

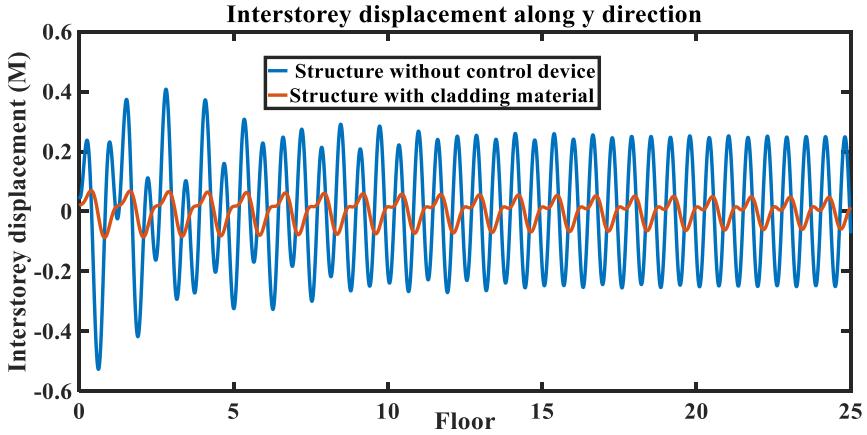

(b). Reduction of inter storey displacement of structural system by using cladding material along y directions

Fig. 13. Reduction of inter storey displacement of a structural system by cladding material.

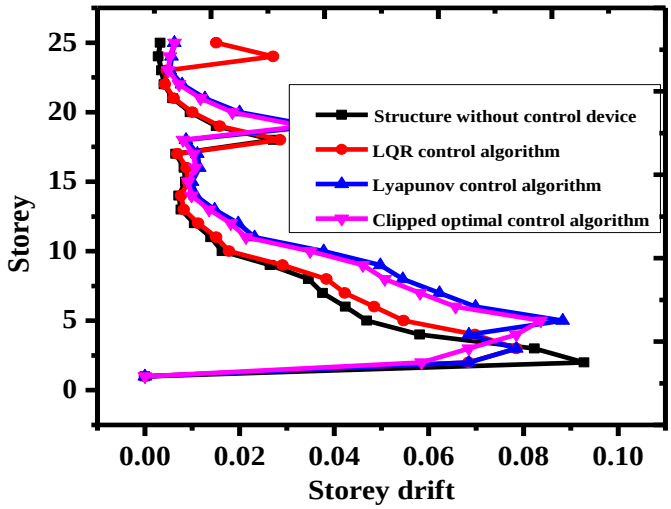

(a). Reduction of Storey drift of structural system by using control device along x directions in 2D

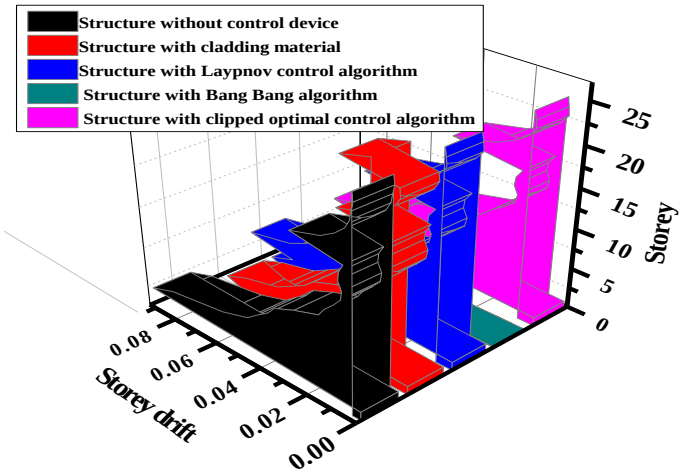

(b). Reduction of Storey drift of structural system by using control device along x directions in 3D

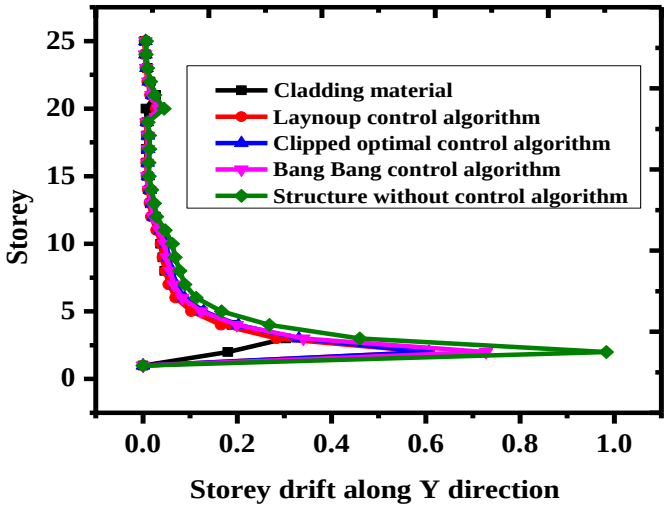

(c). Reduction of Storey drift of structural system by using control device along y directions in 2D

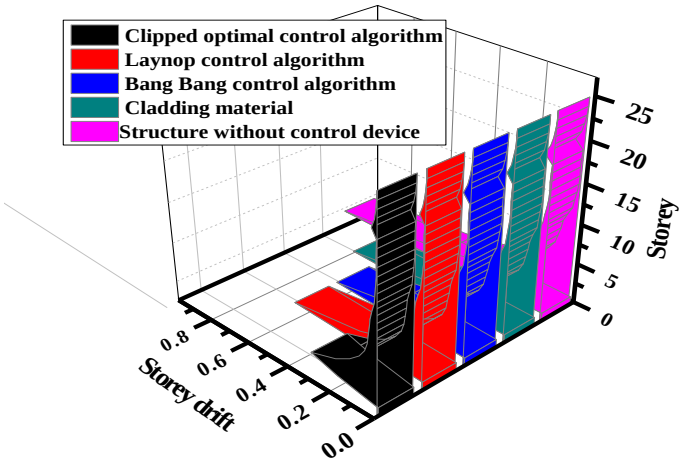

(d). Reduction of Story drift of structural system by using control device along y directions in 3D

Fig. 14. Reduction of story drift of a structural system by using control device.

Figure 15 shows the non-dimensional parameter of the story drift ratio along x and y directions reductions by using cladding and different algorithm of MR damper.

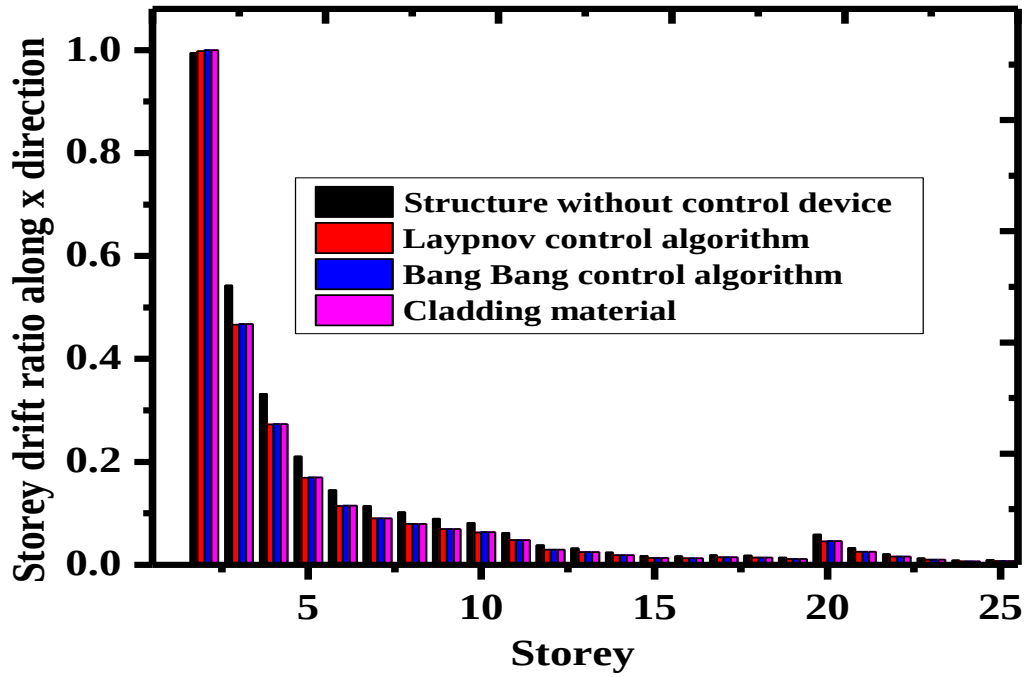

(a). Reduction of Story drift ratio of structural system by using control device along x directions

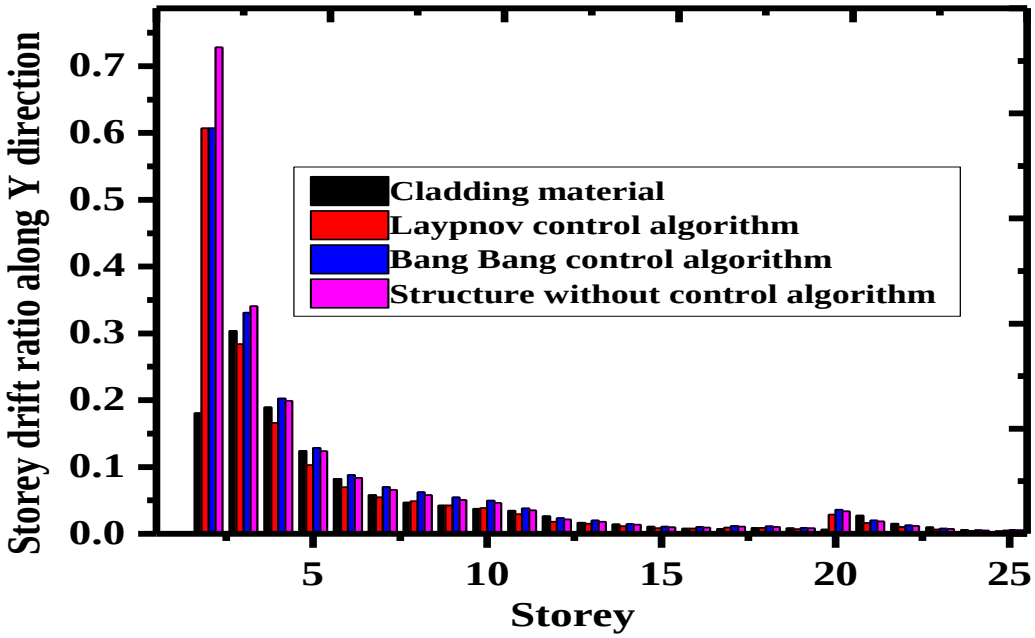

(b). Reduction of Story drift ratio of structural system by using control device along y directions

Fig. 15. Reduction of story drift ratio of a structural system by using control device.

Figure 16 shows the reductions of base shear reductions along x and y directions by using different control algorithm of M.R. damper and cladding material.

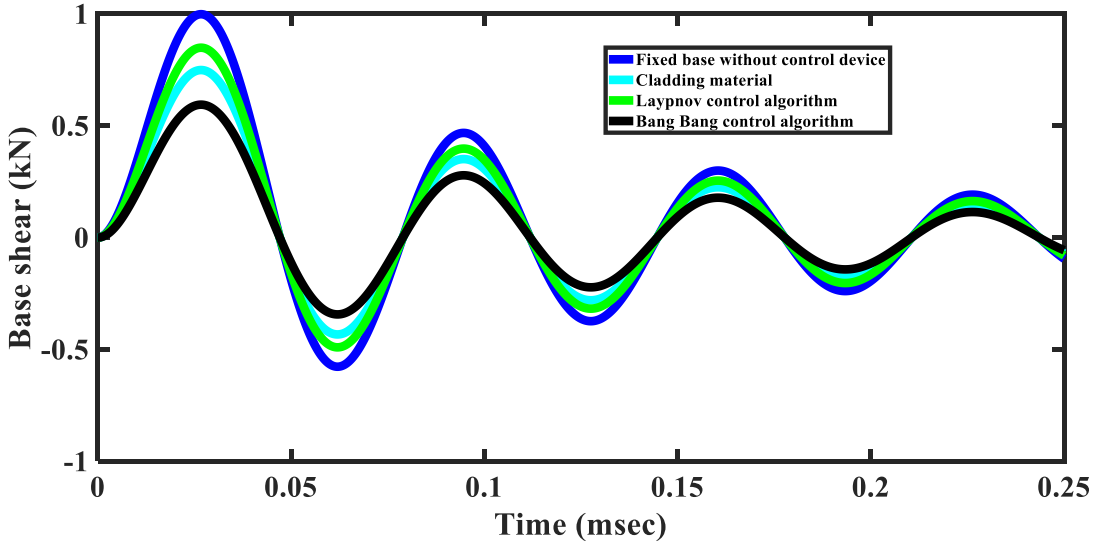

(a). Reduction of base shear of structural system by using control device along x directions

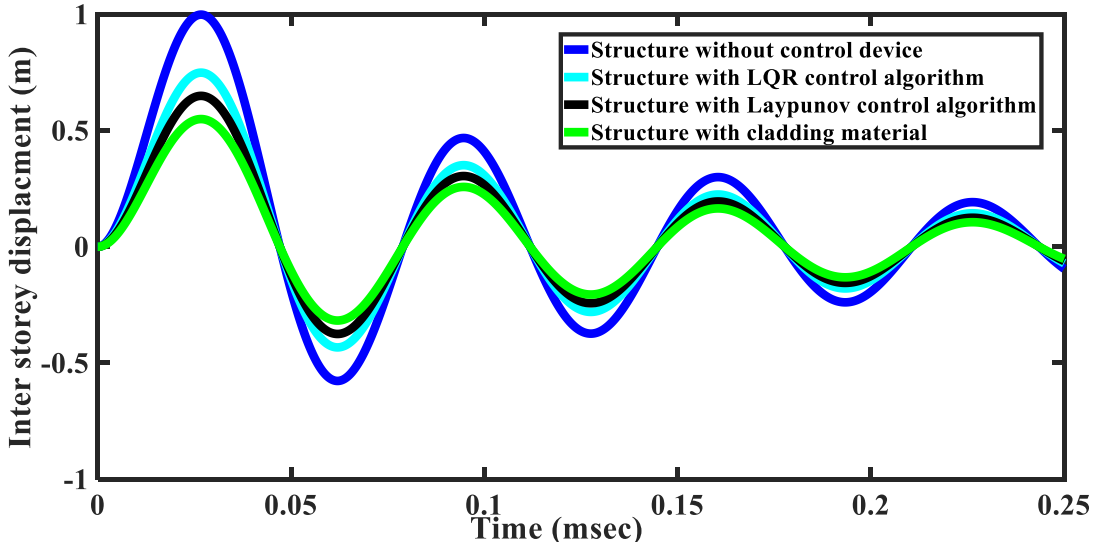

(b). Reduction of base shear of structural system by using control device along y directions

Fig. 16. Reduction of base shear of a structural system by using control device.

Figure 17 shows the increase of the normalized pressure and impulse curve at twenty fourth floor and fifteenth floor along x and y directions by using various M.R. damper. At twenty fourth floor the 0.01 kPa is increases to 0.012 kPa, 0.015 kPa and 0.02 kPa , at fifteenth floor 0.03 kPa is increase to 0.04 kPa, 0.08kpa and 0.098 kPa by using the Lyapunov control algorithm, Bang Bang control algorithm , Clipped optimal control algorithm respectively.

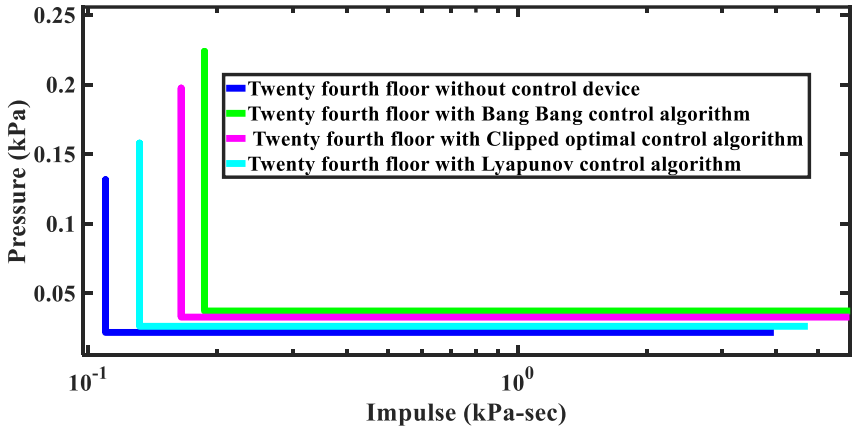

(a). Increase of normalised pressure impulse curve by using control device along x directions

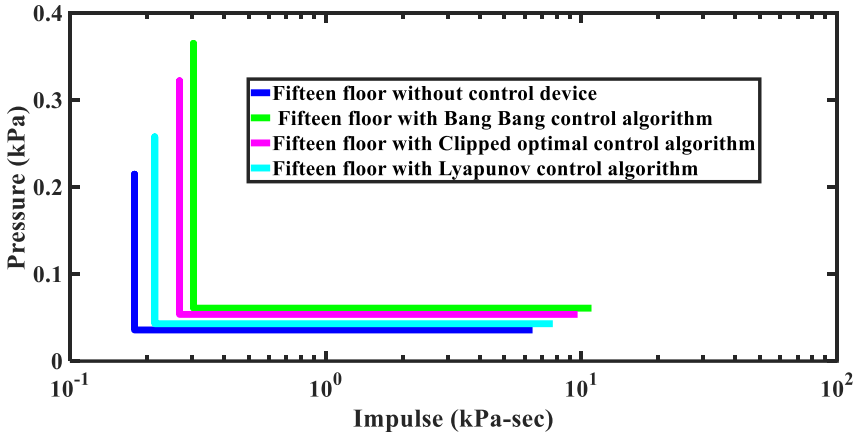

(b). Increase of normalized pressure impulse curve by using control device along y directions

Fig. 17. Increase of normalized pressure impulse curve of a structural system by using control device.

Figure 18 shows the force displacement curve of different current consumptions of MR damper. The maximum force and displacement occur for the current of 2.5A, the minimum force and displacement occurs at 0A.

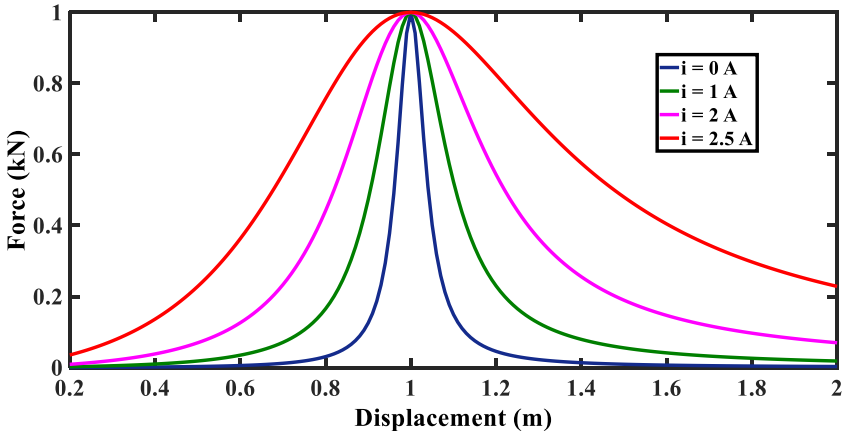

Fig. 18. Deformations of a MR damper with different current.

Figure 19 shows the story drift ratio of the structure with three different mode shape. The mode shape 2 is occurring maximum story drift ratio between the floor 14 to 18 floor. Table 6 and 7 shows the percentage of increase of pressure impulse curve of different algorithm and also energy absorptions.

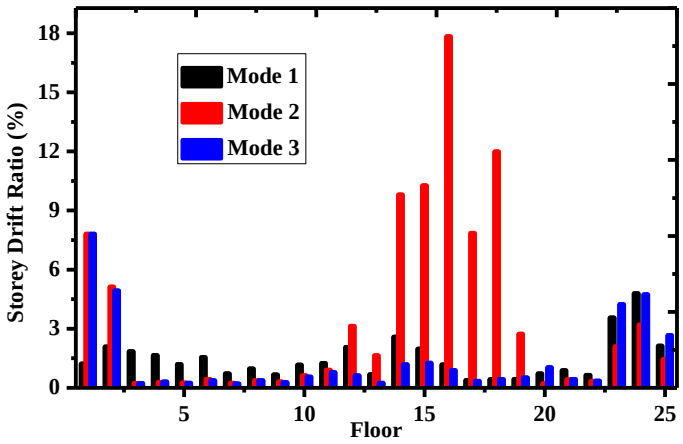

Fig. 19. Story drift ratio of the structural system without control device.

Table 6
Percentage of increase in pressure impulse in each floor by cladding and M.R. damper.

Floor	Pressure (%)				Impulse (%)			
	Cladding material	M.R. damper with different control algorithm			Cladding material	M.R. damper with different control algorithm		
		LQR	Lyapunov	Clipped optimal		LQR	Lyapunov	Clipped optimal
1	20	25	26	78	57	72	54	61
2	22	28	28	76	61	78	48	62
3	25	32	29	65	60	77	73	66
4	28	36	32	68	64	82	63	65
5	19	24	35	75	67	85	25	45
6	16	21	62	72	61	78	56	55
7	33	39	63	74	58	68	45	58
8	41	48	68	70	56	66	68	48
9	66	78	69	64	54	64	66	65
10	65	76	72	65	55	65	62	68
11	55	65	74	78	51	60	60	75
12	58	68	78	76	24	28	61	71
13	64	75	66	65	30	35	52	70
14	61	72	56	68	30	35	55	78
15	63	74	58	75	29	34	56	85
16	60	70	52	56	74	87	58	35
17	54	64	51	58	48	56	60	29
18	55	65	78	57	36	42	61	55
19	51	60	77	55	35	41	38	58
20	49	58	58	78	37	44	47	66
21	41	48	68	89	37	44	44	68
22	56	66	66	68	36	42	45	77
23	53	62	62	59	39	46	49	78
24	66	78	61	62	34	40	50	66
25	70	82	60	61	36	42	51	68

Table 7
Energy absorptions of different control device in different floor.

Floor	Cladding material (J)	Different control algorithm of M.R. damper (J)		
		LQR	Lyapunov	Clipped optimal
1	185	231	270	231
2	186	233	271	233
3	168	210	245	210
4	164	205	239	205
5	158	198	230	198
6	152	190	222	190
7	148	185	216	185
8	142	178	207	178
9	140	175	204	175
10	134	168	195	168
11	132	165	192	165
12	128	160	187	160
13	120	150	175	150
14	115	144	168	144
15	110	138	160	138
16	108	135	157	135
17	104	130	152	130
18	94	118	137	118
19	92	115	134	115
20	85	106	124	106
21	78	98	114	98
22	68	85	99	85
23	64	80	93	80
24	66	83	96	83
25	62	78	90	78

5. Conclusions

The following are the conclusions are drawn based on the results

a. 74.08%, 85.92%, 91.11% and 89.62% reductions of acceleration by cladding material, Bang Bang control algorithm, clipped optimal control algorithm and Lyapunov control algorithm respectively at 3rd floor.76%, 84.4%, 90.4% and 91.2% reductions of acceleration by cladding material, Bang Bang control algorithm, clipped optimal control algorithm and Lyapunov control algorithm respectively at 20th floor.
b. . 27.77%, 25%, 44.44% and 55.55% reductions of acceleration by cladding material, Bang Bang control algorithm, clipped optimal control algorithm and Lyapunov control algorithm respectively at 2nd floor.25%, 43.75%, 43.75% and 50% reductions of acceleration by cladding material, Bang Bang control algorithm, clipped optimal control algorithm and Lyapunov control algorithm respectively at 19th floor.

c. 37.5%, 50%, 70% and 75% reductions of velocity by cladding material, Bang Bang control algorithm, clipped optimal control algorithm and Lyapunov control algorithm respectively at 3rd floor.41.11%, 47.05%, 70.58% and 71.76% reductions of velocity by cladding material, Bang Bang control algorithm, clipped optimal control algorithm and Lyapunov control algorithm respectively at 21th floor.
d. 33.33%, 83.33%, 86.67% and 88.88% reductions of velocity by cladding material, Bang Bang control algorithm, clipped optimal control algorithm and Lyapunov control algorithm respectively at 2nd floor. 25%, 81.25%, 85% and 86.87% reductions of velocity by cladding material, Bang Bang control algorithm, clipped optimal control algorithm and Lyapunov control algorithm respectively at 22 nd floor.
e. 76%, 84%, 92% and 96% reductions of displacement by cladding material, Bang Bang control algorithm, clipped optimal control algorithm and Lyapunov control algorithm respectively at 2nd floor.76%, 84.4%, 90.4% and 91.2% reductions of acceleration by cladding material, Bang Bang control algorithm, clipped optimal control algorithm and Lyapunov control algorithm respectively at 20th floor.
f. Sixteenth floor 45.45%, 40%, 33.33% and 14.29% increases pressure, 34.21%,28.57%, 28.57% and 16.67% increases impulse by using MR damper and cladding material respectively. Fourth floor,
g. 79% and 85% of instorey displacement will be reduced by using cladding material.
h. 12%, 6% , 13% storey drift is reduced , 22%, 28% and 33% is reduced along x and y directions respectively.
i. Maximum story drift ratio occurs at third to seventh floor and minimum story drift ratio occurs at 15 floors to 20 floors.
j. 30%, 40% reductions take place along x and y directions of the base shear by using M.R. damper and cladding material respectively.
k. 45%, 65% and 70% increases normalized pressure without causing failure to the structure
l. The optimum current is consumed by the MR damper are 2.5A.
m. The maximum drift occurs at 2 mode of 13 to 17 floor.
n. The optimizations results show that MR damper is installed at first and second floor plays a vital role in the reduction of the response of a structure system exposed to blast load.
o. Compare to cladding material, MR damper plays a vital role in the reductions of the response of a structural system exposed to blast load.

References

[1] Baker WE, Cox PA, Westline PS, Kulesz JJ, Strehlow RA. Explosion Hazards and Evaluation. Amsterdam, Oxford, New York: Elsevier Scientific Publishing Company 1983.

[2] Jarrett DE. DERIVATION OF THE BRITISH EXPLOSIVES SAFETY DISTANCES. Ann N Y Acad Sci 1968;152:18–35. https://doi.org/10.1111/j.1749-6632.1968.tb11963.x.

[3] Krauthammer T. Modern protective structures. vol. 22. New York: CRC Press; 2008.

[4] Shi Y, Hao H, Li Z-X. Numerical derivation of pressure–impulse diagrams for prediction of RC column damage to blast loads. Int J Impact Eng 2008;35:1213–27. https://doi.org/10.1016/j.ijimpeng.2007.09.001.

[5] Fallah AS, Louca LA. Pressure–impulse diagrams for elastic-plastic-hardening and softening single-degree-of-freedom models subjected to blast loading. Int J Impact Eng 2007;34:823–42. https://doi.org/10.1016/j.ijimpeng.2006.01.007.

[6] Dyke SJ, Spencer Jr BF, Sain MK, Carlson JD. Modeling and control of magnetorheological dampers for seismic response reduction. Smart Mater Struct 1996;5:565–75.

[7] Wells GL. Major hazards and their management. IChemE; 1997.

[8] Gong Y, Cao L, Laflamme S, Ricles J, Quiel S, Taylor D. Motion-based design approach for a novel variable friction cladding connection used in wind hazard mitigation. Eng Struct 2019;181:397–412. https://doi.org/10.1016/j.engstruct.2018.12.033.

[9] Sung S-H, Chong J-W. A fast-running method for blast load prediction shielding by a protective barrier. Def Technol 2020;16:308–15. https://doi.org/10.1016/j.dt.2019.07.011.

[10] Ousji H, Belkassem B, Pyl L, Vantomme J. Air-blast loading on empty metallic beverage can used as sacrificial cladding: Experimental, analytical and numerical study. Eng Struct 2020;204:109979. https://doi.org/10.1016/j.engstruct.2019.109979.

[11] Yanik A. Seismic control performance indices for magneto-rheological dampers considering simple soil-structure interaction. Soil Dyn Earthq Eng 2020;129:105964. https://doi.org/10.1016/j.soildyn.2019.105964.